

Cite this: *Chem. Sci.*, 2022, 13, 9755

All publication charges for this article have been paid for by the Royal Society of Chemistry

Received 1st April 2022  
Accepted 27th July 2022

DOI: 10.1039/d2sc01895k

rsc.li/chemical-science

# The curious case of a sterically crowded Stenhouse salt†

Valentin Théry,<sup>a</sup> Florian Molton,<sup>a</sup> Selim Sirach,<sup>a</sup> Neven Tillet,<sup>a</sup> Jacques Pécaut,<sup>b</sup> Eder Tomás-Mendivil<sup>\*a</sup> and David Martin<sup>†b</sup>\*

We report a peculiar Stenhouse salt. It does not evolve into cyclopentenones upon basification, due to the steric hindrance of its bulky stable carbene patterns. This allowed for the observation and characterization of the transient open-chain neutral derivative, which was isolated as its cyclized form. The latter features an unusually long reactive C–O bond (150 pm) and a rich electrochemistry, including oxidation into an air-persistent radical cation.

## Introduction

In 1850, John Stenhouse observed that furfural-containing oils deeply stain various organic tissues.<sup>1</sup> He later succeeded in crystallising the salt resulting from the addition of aniline to crude furfural in the presence of hydrochloric acid, obtaining “a mass of beautiful iridescent fur”.<sup>2</sup> Despite this simple synthesis, the chemistry of so-called Stenhouse salts  $\mathbf{A}\cdot\mathbf{H}^+$  (Scheme 1) has remained fairly unexplored. Sporadic interest revivals have been limited for a long time by a lack of selectivity and reproducibility.<sup>3</sup> In recent literature, Stenhouse salts are mostly invoked either as (i) formal parent structures for derivative “donor-acceptor Stenhouse adducts” with photo-switching properties,<sup>4</sup> (ii) coloured Maillard-type products in food browning reactions<sup>5</sup> or (iii) elusive intermediates in the formation of cyclopentenones.<sup>6,7</sup> In fact, only a few conditions and substitution patterns (aryl and H, Me or indole as N,N'-substituents)<sup>3h,j,k,6,7a</sup> have allowed the isolation of defined salts  $\mathbf{A}\cdot\mathbf{H}^+$ . They easily evolve into cyclopentenones  $\mathbf{B}$ , which can be substituted with a variety of nucleophiles or rearrange into a more stable isomer  $\mathbf{C}$ .

The neutral deprotonated forms  $\mathbf{A}$  have eluded spectroscopic observation to date. Li and Batey proposed that these intermediates exist in solution as cyclic  $\mathbf{c}\text{-}\mathbf{A}$ , whose ring opening affords less stable  $\mathbf{o}\text{-}\mathbf{A}$ , undergoing fast conrotatory electrocyclicization to give cyclopentenones  $\mathbf{B}$ .<sup>6,7a</sup> Note that the formation of  $\mathbf{B}$  from  $\mathbf{A}\cdot\mathbf{H}^+$  is reversible. In some cases, the addition of acids to  $\mathbf{B}$  gives back  $\mathbf{A}\cdot\mathbf{H}^+$ . For this reason,  $\mathbf{B}$  has been sometimes misattributed to  $\mathbf{A}$ , causing confusion in the research community.<sup>3,7</sup>

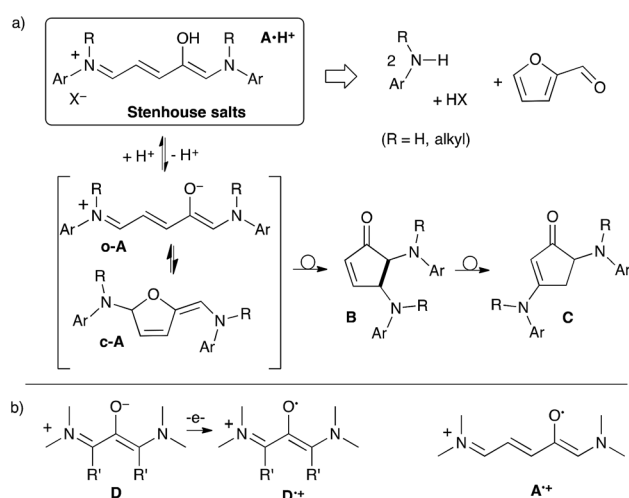
<sup>a</sup>Univ. Grenoble Alpes, CNRS, DCM, Grenoble 38000, France

<sup>b</sup>Univ. Grenoble Alpes, CEA, CNRS, INAC-SyMMES, UMR 5819, Grenoble 38000, France

† Electronic supplementary information (ESI) available. Experimental procedures, characterization data and DFT studies. CCDC 2163356–2163359. For ESI and crystallographic data in CIF or other electronic format see <https://doi.org/10.1039/d2sc01895k>

Open-chain  $\mathbf{o}\text{-}\mathbf{A}$  are reminiscent of 1,3-di(amino)oxyallyls  $\mathbf{D}$ . These diradicaloids have lifetimes from seconds to years in solution at room temperature, depending on substitution patterns.<sup>8,9</sup> We recently reported air-stable versions.<sup>8g</sup> Compounds  $\mathbf{D}$  undergo reversible electron transfers. They afford radical cations  $\mathbf{D}^{\cdot+}$ , which are usually air-persistent. Naturally, we wondered whether vinylogous open-chain  $\mathbf{o}\text{-}\mathbf{A}$  could feature similar redox behaviours. In principle the design of sterically hindered models may prevent the electrocyclization of  $\mathbf{A}\cdot\mathbf{H}^+$  into  $\mathbf{B}$ .

Herein, we describe the synthesis of such a Stenhouse salt featuring the extreme bulky environment provided by a cyclic (alkyl)(amino)carbene (CAAC).<sup>10–12</sup> This allowed for the unprecedented isolation of the cyclic deprotonated derivative  $\mathbf{c}\text{-}\mathbf{A}$  and the spectroscopic observation of its open-chain counterpart  $\mathbf{o}\text{-}\mathbf{A}$ .



**Scheme 1** a) Stenhouse salts  $\mathbf{A}\cdot\mathbf{H}^+$  and their conversion into cyclopentenones. (b) 1,3-Di(amino)oxyallyls  $\mathbf{D}$ , stabilized radical cations  $\mathbf{D}^{\cdot+}$  and putative vinylogous Stenhouse-type  $\mathbf{A}^{\cdot+}$ .



These peculiar Stenhouse-type compounds feature rich redox chemistry, including the oxidation into open-chain  $A^+$ , a persistent paramagnetic cyanine dye.

## Results and discussion

Our approach towards Stenhouse derivatives from a stable carbene involves (i) the formation of an acylium from the addition of a CAAC to an acryloyl chloride,<sup>11</sup> followed by (ii) the 1,4-addition of a second carbene to the resulting Michael acceptor, yielding a Stenhouse salt after proton migration (Scheme 2a). As aminocarbenes are strong bases, it seemed likely that deprotonation to afford **A** would immediately follow. Therefore, we added three equivalents of CAAC to a solution of cinnamoyl chloride in THF. After work-up to remove iminium salts stemming from the protonation of one equivalent of CAAC, a pale-yellow solid was isolated in 44% yield (Scheme 2b). A single-crystal X-ray diffraction study<sup>13</sup> showed the formation of a neutral close-chain Stenhouse derivative **c-1**. Data from <sup>13</sup>C and <sup>1</sup>H NMR spectra are fully consistent. As expected from the low-symmetry of the molecule, all carbons and protons of the 2,6-di(isopropyl)phenyl group (Dipp) and the *gem*-dimethyl and CH<sub>2</sub> protons of the five-membered ring of both CAAC patterns are diastereotopic. Some aromatic protons and isopropyl signals feature unusual up-field <sup>1</sup>H chemical shifts because the rigid structure of **c-1** forces the respective shielding cones of the phenyl and Dipp groups into close proximity.

No trace impurity in isotropic NMR spectra could be attributed to open-chain **o-1**. However, the solid-state structure of **c-1** (Fig. 1) features a remarkably long C1–O1 bond length (150.7 pm). Significant deviation from the standard value (143 pm<sup>14</sup>) is not common for C<sub>sp</sub><sup>3</sup>–O bond lengths, even in strained epoxides,<sup>15</sup> and “extreme” lengths above 150 pm are mostly limited

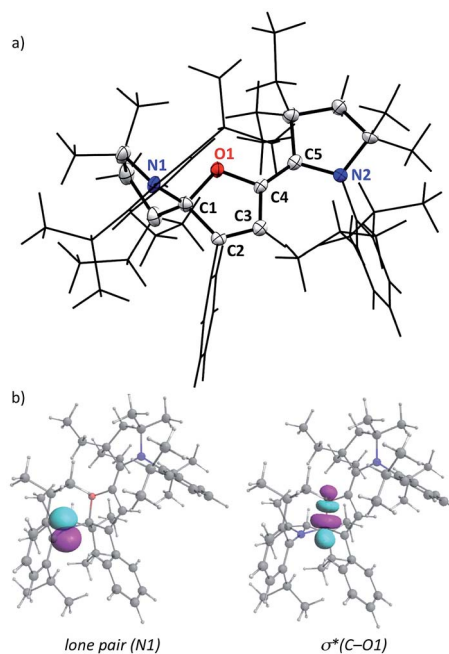
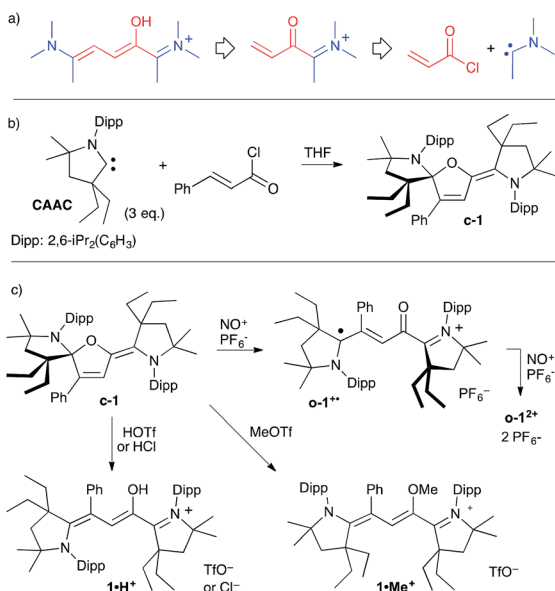


Fig. 1 a) Representation of the single crystal X-ray structure of **c-1**. A wireframe display was used for clarity, with thermal ellipsoids (50% probability) shown only for selected atoms. (b) Representation of relevant natural bond orbitals for **c-1**.

to some reactive oxoniums.<sup>16,17</sup> We ruled out a possible artefact due to interactions or packing effects in the crystal. Indeed, DFT-optimized structures<sup>18,19</sup> corroborated the experimental solid-state geometry (see the ESI<sup>†</sup>), including the shorter C4–O1 distance (139.1 pm, a typical value for single C<sub>sp</sub><sup>2</sup>–O bonds<sup>14</sup>). We found that NBO formalism can account for the unusual elongation of C1–O1. Second-order perturbative energy analysis revealed a strong negative hyperconjugation of the lone pair of N1 into the low-lying  $\sigma^*$ (C1–O1) bond ( $E_{(2)} = 21 \text{ kcal mol}^{-1}$ ). As the cleavage of the weak C1–O1 bond led to **o-1**, this suggested that the reactivity of **c-1** could mimic that of its open-chain counterpart.

Compound **c-1** is sensitive and affords highly coloured compounds when exposed to air or moisture. The hydrolysis product features a strong UV-vis absorption at 526 nm and was identified as the open-chain protonated product **1·H<sup>+</sup>**. It was synthesized by the addition of trifluoromethanesulfonic acid to **c-1**. Stenhouse salt [**1·H<sup>+</sup>**][OTf<sup>−</sup>] is a deep pink to violet iridescent solid with a golden shine (Scheme 2c). Initial crystallization attempts afforded nearly-bidimensional plates (monoclinic, *I2/a*), which could only provide a poorly resolved crystallographic structure determination. Thus, we synthesized [**1·H<sup>+</sup>**][Cl<sup>−</sup>] from the reaction of **c-1** with a solution of HCl in diethylether. Satisfyingly, this chloride salt crystallized as well-defined needles (monoclinic, *P2<sub>1</sub>/c*).

Single-crystal X-ray crystallography confirmed the open-chain structure of **1·H<sup>+</sup>**. In the solid state, the chain is twisted and not fully conjugated, with one dominating resonance structure, as represented in Scheme 2. In solution, the <sup>1</sup>H and <sup>13</sup>C spectra showed broad signals at room temperature, which



Scheme 2 a) Retrosynthetic approach for the synthesis of Stenhouse salt derivatives from stable aminocarbenes; synthesis (b) and reactivity (c) of neutral Stenhouse derivative **c-1**.



sharpened at lower temperature, suggesting a significant conformational flexibility for the  $\pi$ -system. As expected, salts of  $\mathbf{1}\cdot\text{H}^+$  yielded back  $\mathbf{c}\text{-1}$  upon addition of triethylamine. Similarly, addition of methyltriflate (MeOTf) to  $\mathbf{c}\text{-1}$  afforded the *O*-methylated Stenhouse salt  $[\mathbf{1}\cdot\text{Me}^+][\text{OTf}^-]$ , which was fully characterized, including a single-crystal X-ray crystallography study.

EPR of aerated solutions evidenced the presence of a persistent radical, which was attributed to  $\mathbf{o}\text{-1}^{\bullet+}$ . This was confirmed by stoichiometric preparations, either by electrolysis (see further below) or by the reaction of  $\mathbf{c}\text{-1}$  with one equivalent of nitrosonium hexafluorophosphate ( $\text{NO}(\text{PF}_6)$ ) as the oxidant. The radical cation was isolated as a dark red powder (43% yield). It persists in solution for hours. Note that it is rather insensitive to oxygen, with identical half-lives either in air or under an argon atmosphere (about 15 h in acetonitrile at room temperature). Regardless of conditions, it ultimately yielded  $\mathbf{1}\cdot\text{H}^+$ , likely acting as a  $\text{H}^{\bullet}$  scavenger from impurities or solvents. Isotropic EPR hyperfine spectra (Fig. 2) indicated a large hyperfine constant with one hydrogen atom (10 MHz) and only one nitrogen atom (11 MHz).<sup>20</sup> These values were fairly reproduced with DFT calculations (10 and 6 MHz respectively), which also showed that one CAAC moiety is orthogonal to the rest of the  $\pi$ -system, with no significant contribution to the singly occupied molecular orbital (SOMO). As a result, less than 5% Mulliken spin density was found on N2 and C5 (against 20% on O1, 13% on C4, 20% on C3, 13% on C2, 17% on C1 and 17% on N1).

Further oxidation of  $[\mathbf{1}^{\bullet+}][\text{PF}_6^-]$  with a second equivalent of  $\text{NO}(\text{PF}_6)$  led to dication salt  $[\mathbf{1}^{2+}][\text{PF}_6^-]_2$  in 60% yield. It was fully characterized, including a single-crystal X-ray crystallography study.

Cyclic voltammetry experiments unveiled a rich electrochemistry (Fig. 3). Closed-chain  $\mathbf{c}\text{-1}$  undergoes two successive oxidations into  $\mathbf{c}\text{-1}^{\bullet+}$  ( $E^0 = -0.5$  V vs.  $\text{Fc}/\text{Fc}^+$ ) and  $\mathbf{c}\text{-1}^{2+}$  ( $E^0 = -0.16$  V), respectively (processes 1 and 2 in Fig. 3a). A loss of reversibility is observed at a lower scan rate, which was interpreted as the result of ring opening of the oxidized species at room temperature (Fig. 3b). This hypothesis was confirmed by cyclic voltammetry studies of  $[\mathbf{o}\text{-1}^{\bullet+}][\text{PF}_6^-]$ . Indeed, the radical cation undergoes a reversible oxidation at  $E^0 = -0.27$  V to afford  $\mathbf{o}\text{-1}^{2+}$  (process 3). The reduction wave of  $\mathbf{o}\text{-1}^{\bullet+}$  is irreversible at

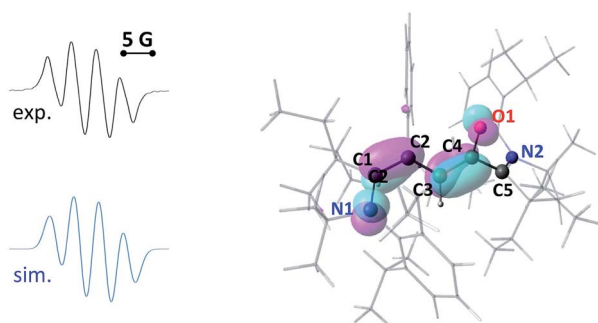


Fig. 2 Left, experimental X-band EPR spectra of  $\mathbf{1}^{\bullet+}$  in acetonitrile at room temperature (black); the corresponding simulated spectra (blue) with the following set of parameters: line-broadening parameter  $lw = 0.288$  and hyperfine coupling constants  $a(^{14}\text{N}) = 11.4$  MHz and  $a(^1\text{H}) = 10.1$  MHz. Right, representation of computed SOMO.

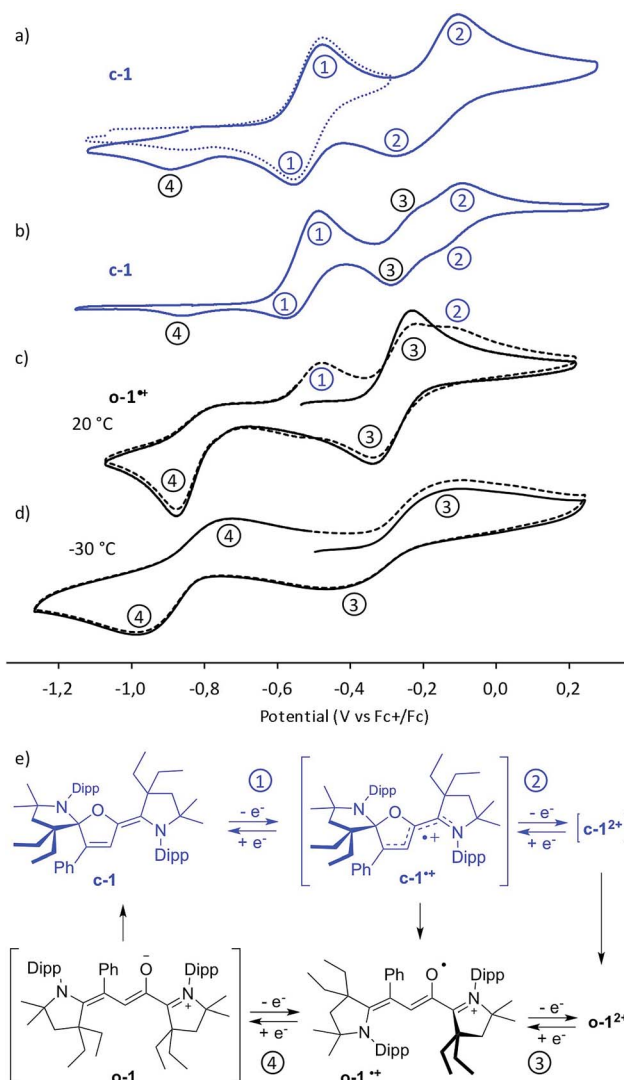


Fig. 3 Cyclic voltammetry at  $100$   $\text{mV s}^{-1}$  rate (if not otherwise stated) with  $0.1$  M  $n\text{Bu}_4\text{NPF}_6$  electrolyte of acetonitrile solution ( $1$  mM) of: (a)  $\mathbf{c}\text{-1}$ , (b)  $\mathbf{c}\text{-1}$  at a rate of  $10$   $\text{mV s}^{-1}$ , (c)  $\mathbf{o}\text{-1}^{\bullet+}$  at  $20$   $^{\circ}\text{C}$ , and (d)  $\mathbf{o}\text{-1}^{\bullet+}$  at  $-30$   $^{\circ}\text{C}$ ; (e) corresponding electrochemical processes.

room temperature, but becomes reversible at  $-30$   $^{\circ}\text{C}$  (process 4,  $E_{1/2} = -0.84$  V), indicating that the fast ring-closure into  $\mathbf{c}\text{-1}$  follows a stepwise EC process with the transient formation of neutral open-chain  $\mathbf{o}\text{-1}$ . Note that after a first reducing cycle in voltammograms of  $[\mathbf{1}^{\bullet+}][\text{PF}_6^-]$ , as  $\mathbf{c}\text{-1}$  is generated, the oxidation waves of  $\mathbf{c}\text{-1}$  into  $\mathbf{c}\text{-1}^{\bullet+}$  (process 1) and  $\mathbf{c}\text{-1}^{\bullet+}$  into  $\mathbf{c}\text{-1}^{2+}$  (process 2) appear. Conversely, this also accounts for cyclic voltammograms of  $\mathbf{c}\text{-1}$  at a low scan-rate, which feature the reduction waves of  $\mathbf{o}\text{-1}^{2+}$  into  $\mathbf{o}\text{-1}^{\bullet+}$  (process 3) and of  $\mathbf{o}\text{-1}^{\bullet+}$  into  $\mathbf{c}\text{-1}$  (process 4).

Cyclic voltammetry experiments indicated that the ring opening of  $\mathbf{c}\text{-1}^{\bullet+}$  was slow enough to allow for its spectroscopic observation. However, UV-monitoring of the electrolysis of  $\mathbf{c}\text{-1}$  couldn't clearly evidence the transient formation of this radical. We realized that the characteristic signals for  $\mathbf{c}\text{-1}^{\bullet+}$  must be hidden by the spectra of  $\mathbf{o}\text{-1}^{\bullet+}$ . Indeed TD-DFT calculations predicted very similar absorptions for both radicals ( $\mathbf{c}\text{-1}^{\bullet+}$ , 560



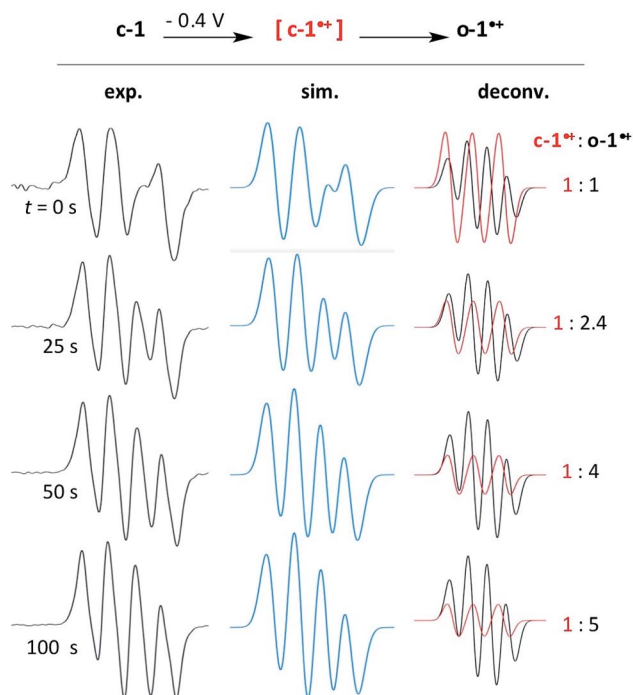


Fig. 4 Left, EPR monitoring of the electrolysis at  $-0.4$  V of **c-1** in acetonitrile; middle, the corresponding simulated spectra; right, deconvolution and respective contribution of **c-1** $\cdot^+$  (red) and **o-1** $\cdot^+$  (black) radicals to the spectra.

and 450 nm; **o-1** $\cdot^+$ , 630 and 430 nm). Thus, we turned to the *in situ* EPR-monitoring of the electrolysis of **c-1** at  $-0.4$  V with an in-house device (see the ESI $^\dagger$ ). We observed the formation of a transient radical with **o-1** $\cdot^+$  (Fig. 4). Note that DFT calculations predicted a simple hyperfine structure for the isotropic EPR spectra of **c-1** $\cdot^+$  (with only a significant coupling constant of 13 MHz with N2). Accordingly, the EPR spectra of the mixtures could be fitted with a close value (15.5 MHz).

Importantly, electrochemical data also showed that the spectroscopic observation of neutral open-chain **o-1**, an elusive derivative of Stenhouse salts to date, could be possible at low temperature. Thus, we performed the addition of a strong base

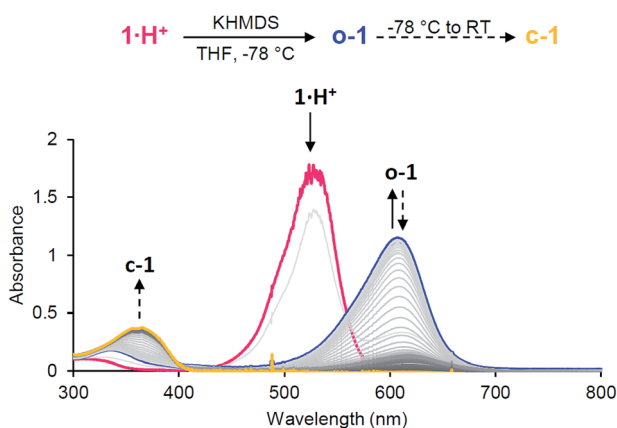


Fig. 5 UV-monitoring of the addition of KHMDS to **1** $\cdot\text{H}^+$  in THF.

(potassium hexamethyldisilazide, KHMDS) to a THF solution of **1** $\cdot\text{H}^+$  at  $-78$  °C. UV-monitoring indicated an instantaneous reaction with the formation of a deep blue compound (Fig. 5). The observation of a strong absorption at 610 nm matched the TD-DFT predictions for **o-1** (608 nm;  $\pi_{\text{HOMO}} \rightarrow \pi_{\text{LUMO}}^*$ ). This band gradually disappeared upon warming to room temperature, as the characteristic band for **c-1** at 358 nm grew.

## Conclusions

The basification of **1** $\cdot\text{H}^+$  yields neutral spirocyclic **c-1**. Such hydrofurans have been previously only considered as elusive intermediates on the route from Stenhouse salts to cyclopentenones. Molecule **c-1** features a remarkably long C–O bond (150.7 pm), typical of those in reactive oxoniums. NBO analysis indicates a strong  $\pi$ -back donation of the lone pair of an amino group into the  $\sigma_{\text{XO}}^*$  orbital, thus accounting for the unusual elongation and easy cleavage of this bond. Neutral **c-1** can undergo two reversible oxidations affording open-chain radical cation **o-1** $\cdot^+$  and dication **o-1** $^{2+}$ . All transient forms of **c-1** (**c-1** $\cdot^+$  and **c-1** $^{2+}$ , as well as zwitterionic **o-1**) could be characterized prior to their respective ring opening or closure.

Open-chain derivatives of **1** stand out among the usual cyanine polymethines.<sup>21</sup> Indeed, the electrochemistry of typical representatives of this large family of organic dyes is mostly limited to one electron-oxidation, yielding short-lived radical dications followed by their fast dimerization or decay.<sup>22</sup> This is in marked contrast with the rich redox behaviour of derivatives **1**. For instance cyanine-based radical **o-1** $\cdot^+$  is air-persistent and its oxidation affords stable dication **o-1** $^{2+}$ . Upon one-electron reduction, the deep-red radical **o-1** $\cdot^+$  is reversibly switched to yellow hydrofuran **c-1**. In turn, reversible protonation can switch **c-1** to deep-pink cyanine **1** $\cdot\text{H}^+$ .

The steric hindrance of the CAAC pattern of the novel Stenhouse derivatives has manifold implications. As already mentioned, it forbids the cyclisation into the corresponding cyclopentenone. It also considerably slows down conformational evolution of the derivatives, as demonstrated by fluxional  $^1\text{H}$  NMR spectroscopy of **1** $\cdot\text{H}^+$  and **1** $\cdot\text{Me}^+$  at room temperature. It is likely for the same reason that the ring-opening of **c-1** $\cdot^+$  and **c-1** $^{2+}$  and ring-closure of **o-1** are remarkably slow intramolecular processes (at least a few seconds at room temperature). Furthermore, steric hindrance prevents optimal conjugation of open-chain derivatives of **1**, which all feature twisted systems. Thus, it is clear that fine-tuning of sterics will significantly impact the electronic, spectroscopic and electrochemical properties of the compounds. We envision that the variety of available stable N-heterocyclic carbenes will allow for the development of a large and diverse family of novel switchable redox-active cyanine dyes.

## Author contributions

D. M. and E. T. M. co-wrote the paper and conceived and designed the study. V. T., F. M., N. T., S. S., D. M. and E. T. M. performed the chemical experiments and analysed the data. D. M. performed the DFT studies. J. P. performed the



crystallographic studies. All authors discussed the results and commented on the manuscript.

## Data availability

The experimental procedures, analytical data and computational details supporting the findings of this study are available within the manuscript and its ESI file.† Raw and unprocessed NMR data are available from the corresponding author upon reasonable request.

## Conflicts of interest

There are no conflicts to declare.

## Acknowledgements

This project has received funding from the European Union's Horizon 2020 research and innovation programme under the Marie Skłodowska-Curie grant agreement no 892162. We acknowledge the CNRS and the University of Grenoble Alpes for a frictionless environment in the context of the Labex Arcane and CBH-EUR-GS (ANR-17-EURE-0003). The authors thank the CECCIC centre of Grenoble for computer resources and the ICMG analytic platform, especially P. Girard, D. Gatineau, R. Sanahuges and N. Altounian for their outstanding service.

## Notes and references

- 1 J. Stenhouse, *Liebigs Ann.*, 1850, **74**, 278–297.
- 2 J. Stenhouse, *Liebigs Ann.*, 1870, **156**, 197–205.
- 3 (a) W. König, K. Hey, F. Schulze, E. Silberkweit and K. Trautmann, *Ber. Dtsch. Chem. Ges.*, 1934, **67**, 1274–1296; (b) G. Williams and C. L. Wilson, *J. Chem. Soc.*, 1942, 506–507; (c) A. P. Dillon and K. G. Lewis, *Tetrahedron*, 1969, **25**, 2035–2039; (d) K. G. Lewis and C. E. Mulquiney, *Aust. J. Chem.*, 1970, **23**, 2315–2323; (e) K. G. Lewis, *Aust. J. Chem.*, 1973, **26**, 893–897; (f) K. G. Lewis and C. E. Mulquiney, *Tetrahedron*, 1977, **33**, 463–475; (g) K. G. Lewis and C. E. Mulquiney, *Aust. J. Chem.*, 1979, **32**, 1079–1092; (h) K. Honda, H. Komizu and M. Kawasaki, *J. Chem. Soc., Chem. Commun.*, 1982, 253–254; (i) B. R. d'Arcy, K. G. Lewis and C. E. Mulquiney, *Aust. J. Chem.*, 1985, **38**, 953–965; (j) P. Šafář and J. Kováč, *Collect. Czech. Chem. Commun.*, 1989, **54**, 2425–2432; (k) H. S. Patel and G. H. Majmudar, *Eur. Polym. J.*, 1991, **27**, 89–92.
- 4 (a) M. M. Lerch, W. Szymański and B. L. Feringa, *Chem. Soc. Rev.*, 2018, **47**, 1910–1937; (b) S. Helmy, F. A. Leibfarth, S. Oh, J. E. Poelma, C. J. Hawker and J. Read de Alaniz, *J. Am. Chem. Soc.*, 2014, **136**, 8169–8172; (c) S. Helmy, S. Oh, F. A. Leibfarth, C. J. Hawker and J. Read de Alaniz, *J. Org. Chem.*, 2014, **79**, 11316–11329.
- 5 T. Hofmann, *J. Agric. Food Chem.*, 1998, **46**, 932–940.
- 6 R. F. A. Gomes, J. A. S. Coelho and C. A. M. Afonso, *Chem. – Eur. J.*, 2018, **24**, 9170–9186.
- 7 (a) S.-W. Li and R. A. Batey, *Chem. Commun.*, 2007, **43**, 3759–3761; (b) A. Procopio, P. Costanzo, M. Curini, M. Nardi, M. Oliverio and G. Sindona, *ACS Sustainable Chem. Eng.*, 2013, **1**, 541–544; (c) K. Griffiths, C. W. D. Gallop, A. Abdul-Sada, A. Vargas, O. Navarro and G. E. Kostakis, *Chem. – Eur. J.*, 2015, **21**, 6358–6361; (d) K. Griffiths, P. Kumar, J. D. Mattock, A. Abdul-Sada, M. B. Pitak, S. J. Coles, O. Navarro, A. Vargas and G. E. Kostakis, *Inorg. Chem.*, 2016, **55**, 6988–6994; (e) M. S. Estevão, R. J. V. Martins and C. A. M. Afonso, *J. Chem. Educ.*, 2017, **94**, 1587–1589; (f) R. F. A. Gomes, N. R. Esteves, J. A. S. Coelho and C. A. M. Afonso, *J. Org. Chem.*, 2018, **83**, 7509–7513; (g) M. L. Di Gioia, M. Nardi, P. Costanzo, A. De Nino, L. Maiuolo, M. Oliverio and A. Procopio, *Molecules*, 2018, **23**, 1891–1904; (h) S. I. Sampani, A. McGown, A. Vargas, A. Abdul-Sada, G. J. Tizzard, S. J. Coles, J. Spencer and G. E. Kostakis, *J. Org. Chem.*, 2019, **84**, 6858–6867; (i) J. G. Pereira, J. P. M. António, R. Mendonça, R. F. A. Gomes and C. A. M. Afonso, *Green Chem.*, 2020, **22**, 7484–7490; (j) K. Peewasan, M. P. Merkel, O. Fuhr and A. K. Powell, *Dalton Trans.*, 2020, **49**, 2331–2336; (k) T. B. Shah, R. S. Shiny, R. B. Dixit and B. C. Dixit, *J. Saudi Chem. Soc.*, 2014, **18**, 985–992.
- 8 (a) D. Martin, C. E. Moore, A. L. Rheingold and G. Bertrand, *Angew. Chem., Int. Ed.*, 2013, **52**, 7014–7017; (b) T. Schulz, C. Farber, M. Leibold, C. Bruhn, W. Baumann, D. Selent, T. Porsch, M. C. Holthausen and U. Siemeling, *Chem. Commun.*, 2013, **49**, 6834; (c) V. Regnier and D. Martin, *Org. Chem. Front.*, 2015, **2**, 1536–1545; (d) V. Regnier, F. Molton, C. Philouze and D. Martin, *Chem. Commun.*, 2016, **52**, 11422–11425; (e) M. Devillard, V. Regnier, M. Tripathi and D. Martin, *J. Mol. Struct.*, 2018, **1172**, 3–7; (f) M. Tripathi, V. Regnier, Z. Ziani, M. Devillard, C. Philouze and D. Martin, *RSC Adv.*, 2018, **8**, 38346–38350; (g) E. Tomás-Mendivil, M. Devillard, V. Regnier, J. Pecaut and D. Martin, *Angew. Chem., Int. Ed.*, 2020, **59**, 11516–11520.
- 9 See also: (a) U. Siemeling, C. Farber, C. Bruhn, M. Leibold, D. Selent, W. Baumann, M. von Hopffgarten, C. Goedecke and G. Frenking, *Chem. Sci.*, 2010, **1**, 697; (b) S. D. Ursula and U. Radius, *Organometallics*, 2017, **36**, 1398; (c) G. Kuzmanich, F. Spänig, C. K. Tsai, J. M. Um, R. M. Hoekstra, K. N. Houk, D. M. Guldi and M. A. Garcia-Garibay, *J. Am. Chem. Soc.*, 2011, **133**, 2342.
- 10 (a) V. Lavallo, Y. Canac, C. Prasang, B. Donnadiu and G. Bertrand, *Angew. Chem., Int. Ed.*, 2005, **44**, 5705; (b) M. Melaimi, M. Soleilhavoup and G. Bertrand, *Angew. Chem., Int. Ed.*, 2010, **49**, 8810–8849; (c) M. Soleilhavoup and G. Bertrand, *Acc. Chem. Res.*, 2015, **48**, 256–266; (d) S. Roy, K. C. Mondal and H. W. Roesky, *Acc. Chem. Res.*, 2016, **49**, 357–369; (e) U. S. D. Paul and U. Radius, *Eur. J. Inorg. Chem.*, 2017, 3362–3375; (f) M. Melaimi, R. Jazzar, M. Soleilhavoup and G. Bertrand, *Angew. Chem., Int. Ed.*, 2017, **56**, 10046–10068.
- 11 CAAC-based organic radicals: (a) J. K. Mahoney, D. Martin, C. Moore, A. Rheingold and G. Bertrand, *J. Am. Chem. Soc.*, 2013, **135**, 18766–18769; (b) L. Jin, M. Melaimi, L. L. Liu and G. Bertrand, *Org. Chem. Front.*, 2014, **1**, 351–354; (c) Y. Li, K. C. Mondal, P. P. Samuel, H. Zhu, C. M. Orben, S. Panneerselvam, B. Dittrich, B. Schwederski, W. Kaim,



- T. Mondal, D. Koley and H. W. Roesky, *Angew. Chem., Int. Ed.*, 2014, **53**, 4168–4172; (d) J. K. Mahoney, D. Martin, F. Thomas, C. Moore, A. L. Rheingold and G. Bertrand, *J. Am. Chem. Soc.*, 2015, **137**, 7519–7525; (e) S. Styra, M. Melaimi, C. E. Moore, A. L. Rheingold, T. Augenstein, F. Breher and G. Bertrand, *Chem. – Eur. J.*, 2015, **21**, 8441–8446; (f) D. Munz, J. Chu, M. Melaimi and G. Bertrand, *Angew. Chem., Int. Ed.*, 2016, **55**, 12886–12890; (g) J. K. Mahoney, R. Jazzar, G. Royal, D. Martin and G. Bertrand, *Chem. – Eur. J.*, 2017, **23**, 6206–6212; M. M. Hansmann, M. Melaimi and G. Bertrand, *J. Am. Chem. Soc.*, 2017, **139**, 15620–15623. (i) M. M. Hansmann, M. Melaimi and G. Bertrand, *J. Am. Chem. Soc.*, 2018, **140**, 2206–2213; (j) P. W. Antoni and M. M. Hansmann, *J. Am. Chem. Soc.*, 2018, **140**, 14823–14835; (k) P. W. Antoni, T. Bruckhoff and M. M. Hansmann, *J. Am. Chem. Soc.*, 2019, **141**, 9701–9711; (l) V. Regnier, E. A. Romero, F. Molton, R. Jazzar, G. Bertrand and D. Martin, *J. Am. Chem. Soc.*, 2019, **141**, 1109–1117; (m) J. Messelberger, A. Grünwald, S. J. Goodner, F. Zeilinger, P. Pinter, M. E. Miehllich, F. W. Heinemann, M. M. Hansmann and D. Munz, *Chem. Sci.*, 2020, **11**, 4138–4149.
- 12 For stable organic radicals based on other types of N-heterocyclic carbenes, see also: (a) J. Back, J. Park, Y. Kim, H. Kang, Y. Kim, M. J. Park, K. Kim and E. Lee, *J. Am. Chem. Soc.*, 2017, **139**, 15300–15303; (b) C. L. Dearthoff, R. E. Sikma, C. P. Rhodes and T. W. Hudnall, *Chem. Commun.*, 2016, **52**, 9024–9027; (c) L. Y. M. Eymann, A. G. Tskhovrebov, A. Sienkiewicz, J. L. Bila, I. Zikhovic, H. M. Ronnow, M. D. Wodrich, L. Vannay, C. Corminboeuf, P. Pattison, E. Solari, R. Scopelliti and K. Severin, *J. Am. Chem. Soc.*, 2016, **138**, 15126–15129; (d) D. Rottschäfer, B. Neumann, H.-G. Stämmler, M. van Gastel, D. M. Andrada and R. S. Ghadwal, *Angew. Chem., Int. Ed.*, 2018, **57**, 4765–4768; (e) N. M. Gallagher, H.-Z. Ye, S. Feng, J. Lopez, Y. G. Zhu, T. Van Voorhis, Y. Shao-Horn and J. A. Johnson, *Angew. Chem., Int. Ed.*, 2020, **59**, 3952–3955; (f) Y. Kim, J. E. Byeon, G. Y. Jeong, S. S. Kim, H. Song and E. Lee, *J. Am. Chem. Soc.*, 2021, **143**(23), 8527–8532; (g) J. Zhao, X. Li and Y.-F. Han, *J. Am. Chem. Soc.*, 2021, **143**, 14428–14432; (h) L. Delfau, S. Nichilo, F. Molton, J. Broggi, E. Tomás-Mendivil and D. Martin, *Angew. Chem., Int. Ed.*, 2021, **60**, DOI: [10.1002/anie.202111988](https://doi.org/10.1002/anie.202111988).
- 13 CCDC 2163356–2163359 contains the crystallographic data for this paper. These data are provided free of charge by the Cambridge crystallographic data centre.
- 14 F. H. Allen, O. Kennard, D. G. Watson, L. Brammer, A. G. Orpen and R. Taylor, *J. Chem. Soc., Perkin trans. II*, 1987, S1.
- 15 See for example: A. J. Leyhane and M. L. Snapper, *Org. Lett.*, 2006, **8**, 5183–5186.
- 16 G. Gunbas, N. Hafezi, W. L. Sheppard, M. M. Olmstead, I. V. Stoyanova, F. S. Tham, M. P. Meyer and M. Mascal, *Nat. Chem.*, 2012, **4**, 1018–1023.
- 17 A long C–O bond was also reported in strained acenaphthofurans: Y. Uchimura, T. Shimajiri, Y. Ishigaki, R. Katoono and T. Suzuki, *Chem. Commun.*, 2018, **54**, 10300–10303.
- 18 M. J. Frisch, G. W. Trucks, H. B. Schlegel, G. E. Scuseria, M. A. Robb, J. R. Cheeseman, *et al.*, *Calculations were performed with the Gaussian suite of programs: Gaussian09, Revision D.01*, Gaussian, Inc., Wallingford CT, 2009. See the ESI† for complete citation.
- 19 If not otherwise stated, calculations were carried out at the B3LYP/6-311g(d,p) level of theory with the PCM model for acetonitrile and Grimme's D3 empirical dispersion: S. Grimme, J. Antony, S. Ehrlich and H. Krieg, *J. Chem. Phys.*, 2010, **132**, 154104.
- 20 Experimental values for isotropic hyperfine constants were extracted from EPR spectra by fitting with the EasySpin simulation package: S. Stoll and A. Schweiger, *J. Magn. Reson.*, 2006, **178**, 42–55.
- 21 For general reviews on cyanine dyes: (a) A. Mishra, R. K. Behera, P. K. Behera, B. K. Mishra and G. B. Behera, *Chem. Rev.*, 2000, **100**, 1973–2012; (b) J. L. Bredas, C. Adant, P. Tackx, A. Persoons and B. M. Pierce, *Chem. Rev.*, 1994, **94**, 243–278.
- 22 (a) R. Lenhard and A. D. Cameron, *J. Phys. Chem.*, 1993, **97**, 4916–4925; (b) J. E. H. Buston, F. Marken and H. L. Anderson, *Chem. Commun.*, 2001, **37**, 1046–1047; (c) J. L. Lyon, D. M. Eisele, S. Kirstein, J. P. Rabe, D. A. Vanden Bout and K. J. Stevenson, *J. Phys. Chem. C*, 2008, **112**, 1260–1268; (d) J. Lenhard and R. Parton, *J. Am. Chem. Soc.*, 1987, **109**, 5808–5813; (e) R. Parton and J. Lenhard, *J. Org. Chem.*, 1990, **55**, 49–57.

